



HAL
open science

An Asymmetric Stabilizer Based on Scheduling Shifted Coordinates for Single-Input Linear Systems With Asymmetric Saturation

Philipp Braun, Giulia Giordano, Christopher M Kellett, Luca Zaccarian

► **To cite this version:**

Philipp Braun, Giulia Giordano, Christopher M Kellett, Luca Zaccarian. An Asymmetric Stabilizer Based on Scheduling Shifted Coordinates for Single-Input Linear Systems With Asymmetric Saturation. *IEEE Control Systems Letters*, 2021, 6, pp.746-751. 10.1109/LCSYS.2021.3086216 . hal-03427397

HAL Id: hal-03427397

<https://laas.hal.science/hal-03427397>

Submitted on 13 Nov 2021

HAL is a multi-disciplinary open access archive for the deposit and dissemination of scientific research documents, whether they are published or not. The documents may come from teaching and research institutions in France or abroad, or from public or private research centers.

L'archive ouverte pluridisciplinaire **HAL**, est destinée au dépôt et à la diffusion de documents scientifiques de niveau recherche, publiés ou non, émanant des établissements d'enseignement et de recherche français ou étrangers, des laboratoires publics ou privés.

An asymmetric stabilizer based on scheduling shifted coordinates for single-input linear systems with asymmetric saturation*

Philipp Braun¹ Giulia Giordano² Christopher M. Kellett¹ and Luca Zaccarian^{2,3}

Abstract—Starting from a symmetric state-feedback solution ensuring α -exponential convergence in an ellipsoidal sublevel set, with asymmetric saturation and single-input linear plants, we propose a novel asymmetric scheduled extension preserving the original symmetric solution in that sublevel set and extending the guaranteed stability region to the union of all possible contractive ellipsoids centered at a shifted equilibrium. Our design being based on the solution of a parametric optimization problem, we prove continuity properties of the ensuing feedback law and we compute its explicit state-feedback expression.

I. INTRODUCTION

While historically input saturation has been mostly studied using symmetric limits (see, e.g., [6], [12]), recent technological challenges show that asymmetric limits often arise in practice, thereby making the symmetric solutions (typically based on focusing at the smallest limit) quite conservative.

As a consequence, the community started looking into nonsymmetric Lyapunov certificates in the presence of symmetric stabilizers (see [1] and references therein, and also [7], [8]). Additionally, [9] and [5] use a piecewise quadratic Lyapunov function with symmetric stabilizing saturated linear feedbacks, in the continuous-time and discrete-time cases, respectively. Alternative recent techniques include symmetrically stabilizing a shifted equilibrium (see [2, ch. 8] and references therein), but this comes at the cost of not stabilizing the origin any longer. Finally, more sophisticated stabilizers have been proposed in [13], where a switching dynamical controller is designed, capable of exploiting the available range of the control action on both sides of the saturation levels. In an attempt to provide enlarged regions of attraction, we recently proposed in [10] the design of an asymmetric stabilizer, based on the convex scaling proposed in [3] for the shifted stabilizer. That solution provides significantly larger guarantees but has the drawback of 1) restricting the achievable region of attraction with a conservative point inclusion condition required to apply the technique in [3] and 2) reducing the local performance of the symmetric solution.

In this work we propose a novel asymmetric scheme based on focusing on the shifted equilibrium, as in [2, ch. 8], and continuously driving that equilibrium back to the origin by

relying on the solution of a parametric optimization problem. As compared to [10], this solution is not based on convex scalings and therefore preserves the convergence rate given by the symmetric stabilizer in its guaranteed ellipsoidal set. Moreover, it does not require any point inclusion conditions, therefore obtaining an estimate of the basin of attraction containing all the contractive ellipsoids that can be constructed in shifted coordinates. While the proposed framework applies to multi-input plants, we focus most of the paper on the single-input case, for which we can compute explicit expressions of the control law solving the optimization. In the rest of the paper we discuss symmetric and shifted asymmetric stabilizers in Section II, then for the single-input case we propose our optimization-based solution in Section III and its explicit version in Section IV. Numerical examples in Section V show the ability of our controller to provide greatly enlarged certified stability regions.

Notation. For $u^-, u^+ \in \mathbb{R}_{\geq 0}^m$, $m \in \mathbb{N}$, $\text{sat}_{[u^-, u^+]}(u) = \max\{\min\{u^+, u\}, -u^-\}$ defines the saturation, where the maximum/minimum are to be understood componentwise. The deadzone is defined through $\text{dz}_{[u^-, u^+]}(u) = u - \text{sat}_{[u^-, u^+]}(u)$. For $Z \in \mathbb{R}^{n \times n}$, $\text{He}(\cdot)$ denotes the function $\text{He}(Z) = Z + Z^\top$. For $Z \in \mathbb{R}^{n \times m}$ and $z \in \mathbb{R}^n$, $Z_{[k]}$ and z_k denote the k -th row and the k -th entry, respectively. A vector $v \in \mathbb{R}^n$ satisfies $v \leq \min\{u^-, u^+\}$ if $v_k \leq u_k^-$ and $v_k \leq u_k^+$ for all $k \in \mathbb{N}$. A symmetric positive definite matrix $P \in \mathbb{R}^{n \times n}$ can be uniquely decomposed as $P = P^{\frac{1}{2}} P^{\frac{1}{2}}$ where $P^{\frac{1}{2}} \in \mathbb{R}^{n \times n}$ is symmetric and positive definite. We use the norms $|x| = \sqrt{x^\top x}$, $x \in \mathbb{R}^n$, and $|x|_P = \sqrt{x^\top P x}$, $P \in \mathbb{R}^{n \times n}$ positive definite. Finally, $I \in \mathbb{R}^{n \times n}$ denotes the identity matrix, $\mathbb{1} \in \mathbb{R}^n$ satisfies $\mathbb{1}_k = 1$, $k \in \{1, \dots, n\}$ and $\text{int}(A)$ denotes the interior of a set $A \subset \mathbb{R}^n$.

II. SYMMETRIC AND SHIFTED STABILIZERS

We consider linear saturated continuous time systems

$$\dot{x} = Ax + B \text{sat}_{[u^-, u^+]}(u) \quad (1)$$

with state $x \in \mathbb{R}^n$, input $u \in \mathbb{R}^m$, $A \in \mathbb{R}^{n \times n}$, $B \in \mathbb{R}^{n \times m}$ and saturation limits $u^-, u^+ \in \mathbb{R}_{>0}^m$. We define the average saturation range $\bar{u} \in \mathbb{R}^m$ and the average saturation center $u_o \in \mathbb{R}^m$ as

$$\bar{u} = \frac{1}{2}(u^+ + u^-), \quad u_o = \frac{1}{2}(u^+ - u^-). \quad (2)$$

For simplicity, we assume that the average saturation range \bar{u}_k satisfies $\bar{u}_k = 1$ for all $k \in \{1, \dots, m\}$; this is not restrictive and can always be assumed without loss of generality for $u^-, u^+ \in \mathbb{R}_{>0}^m$ by scaling the columns of B .

* P. Braun and L. Zaccarian are supported in part by the Agence Nationale de la Recherche (ANR) via grant ‘‘Hybrid And Networked Dynamical sYstems’’ (HANDY), number ANR-18-CE40-0010.

¹School of Engineering, Australian National University, Canberra, Australia. philipp.braun@anu.edu.au, chris.kellett@anu.edu.au

²Department of Industrial Engineering, University of Trento, Trento, Italy. giulia.giordano@unitn.it

³LAAS-CNRS, Université de Toulouse, Toulouse, France. luca.zaccarian@laas.fr

Assumption 1: The average saturation range satisfies $\bar{u} = \mathbb{1} \in \mathbb{R}^m$. \diamond

To convey the idea of the controller design and to obtain explicit formulations, we restrict our presentation in most parts of the paper to the single input case and we assume that the matrix A is non-singular. However, by discussing different cases and by using a more convoluted notation, the ideas seem to extend to the multi input case and to dynamics (1) with singular matrix A .

Assumption 2: The pair (A, B) is stabilizable and A is non-singular. \diamond

Of particular interest in this paper is the subspace of induced equilibria

$$\Gamma = \{x_e \in \mathbb{R}^n : Ax_e + Bu_e = 0, u_e \in \mathbb{R}^m\}. \quad (3)$$

Under Assumption 2, there is a continuous mapping $u_e \mapsto x_e(u_e)$ defined as

$$x_e(u_e) = -A^{-1}Bu_e, \quad (4)$$

characterizing pairs of induced equilibria $(x_e, u_e) \in \Gamma \times \mathbb{R}^m$ through the input $u_e \in \mathbb{R}^m$. Note that, in the definition of Γ , the saturation levels are not present. System (1) with $u \in [-u^-, u^+]$ can only be stabilized at x_e if a corresponding input satisfies $u_e \in (-u^-, u^+)$.

In a neighborhood of the origin, we are looking for a feedback law

$$u = Kx + Ldz_{[u^-, u^+]}(u), \quad (5)$$

with $K \in \mathbb{R}^{m \times n}$, $L \in \mathbb{R}^{m \times m}$, asymptotically stabilizing the origin. Combining (1) and (5), the closed loop dynamics can be written as

$$\begin{aligned} \dot{x} &= (A + BK)x - (B - BL)dz_{[u^-, u^+]}(u) \\ u &= Kx + Ldz_{[u^-, u^+]}(u). \end{aligned} \quad (6)$$

To characterize regions of attraction of asymptotically stable (induced) equilibria x_e , we consider sublevel sets of quadratic functions. In particular, for $\kappa \in \mathbb{R}_{\geq 0}$, $x_e \in \mathbb{R}^n$ and $P \in \mathbb{R}^{n \times n}$ positive definite we define the set

$$\mathcal{E}_{x_e}^\kappa(P) = \{x \in \mathbb{R}^n : |x - x_e|_P \leq \kappa\}. \quad (7)$$

Proposition 1 (Symmetric Stabilizer, [10, Theorem 1]):

Given the plant (1), let $v \in \mathbb{R}_{>0}^m$ with $v \leq \min\{u^-, u^+\}$ and let $\alpha \in \mathbb{R}_{\geq 0}$. Moreover, let $\tilde{Q}_v \in \mathbb{R}^{n \times n}$, $W_v, Y_v \in \mathbb{R}^{m \times n}$, $U_v, X_v \in \mathbb{R}^{m \times m}$ be a solution of the optimization problem

$$\max_{Q, W, Y, U, X} \log \det(Q) \quad (8)$$

subject to $U > 0$ diagonal, $Q = Q^\top > 0$

$$\text{He} \begin{bmatrix} AQ + BW + \alpha Q & -BU + BX \\ W + Y & X - U \end{bmatrix} < 0$$

$$\begin{bmatrix} v_k^2 & Y_{[k]} \\ Y_{[k]}^\top & Q \end{bmatrix} \geq 0, \quad k = 1, \dots, m.$$

Then, for

$$K = W_v Q_v^{-1}, \quad L = X_v U_v^{-1}, \quad P_v = Q_v^{-1} \quad (9)$$

the nonlinear algebraic loop in (5) is well posed (i.e., its solution is unique and Lipschitz) and function $x^\top P_v x$ exponentially decreases with rate larger than 2α within the sublevel set $\mathcal{E}_0^1(P_v)$. Consequently, the origin of (6) is locally exponentially stable, with basin of attraction containing the set $\mathcal{E}_0^1(P_v)$. \lrcorner

The subscript v is used to indicate the dependence of P on the selection of vector $v \in \mathbb{R}_{>0}^m$. In particular, we observe that LMIs (8) are homogeneous in the decision variables, except for v_k^2 in the constraints. Therefore, scaling vector v in Proposition 1 by a positive scalar κ leads to scaling the corresponding optimal solution (8) by κ^2 . More specifically, according to (9), this corresponds to a scaled $P_{\kappa v} = \kappa^{-2}P_v$, whereas gains K and L remain unchanged because the scaling cancels out (this is the reason why no subscript is used in K and L). Finally, the certified ellipsoidal set scales from $\mathcal{E}_0^1(P_v)$ to $\mathcal{E}_0^1(P_{\kappa v}) = \mathcal{E}_0^\kappa(P_v)$. This fact is stated in the next corollary.

Corollary 1 (Homogeneity): Let K, L, P_v defined in (9) correspond to an optimal solution of (8) for $v \in \mathbb{R}_{>0}^m$. Then for all $\kappa \in \mathbb{R}_{\geq 0}$ with $\kappa v \leq \min\{u^-, u^+\}$, and with the same gains K and L , function $x^\top P_v x$ exponentially decreases with rate larger than 2α within the set $\mathcal{E}_0^\kappa(P_v)$. \lrcorner

Proposition 1 can be used to define a control law stabilizing an induced equilibrium, instead of the origin. Consider an equilibrium pair (x_e, u_e) satisfying (4) and assume that $u^- + u_e, u^+ - u_e \in \mathbb{R}_{>0}^m$. Additionally, consider the coordinate transformation

$$\tilde{x} = x - x_e \quad \text{and} \quad \tilde{u} = u - u_e.$$

Then, it holds that

$$\begin{aligned} \dot{\tilde{x}} &= \dot{x} = Ax + B \text{sat}_{[u^-, u^+]}(u) \\ &= A\tilde{x} + Ax_e + B \text{sat}_{[u^-, u^+]}(\tilde{u} + u_e) \\ &= A\tilde{x} + Ax_e + B(u_e + \text{sat}_{[u^- + u_e, u^+ - u_e]}(\tilde{u})) \\ &= A\tilde{x} + B \text{sat}_{[u^- + u_e, u^+ - u_e]}(\tilde{u}). \end{aligned} \quad (10a)$$

with the shifted input \tilde{u} selected as follows

$$\tilde{u} = K\tilde{x} + Ldz_{[u^- + u_e, u^+ - u_e]}(\tilde{u}). \quad (10b)$$

For the shifted dynamics (10), it is evident that the same result as that of Corollary 1 applies. This fact is stated in the following corollary, where a more convenient expression of u is deduced from (10b) exploiting the identities (4) and $dz_{[u^- + u_e, u^+ - u_e]}(\tilde{u}) = dz_{[u^-, u^+]}(u)$, which follows straightforwardly from (10a).

Corollary 2: Let Assumption 2 be satisfied. Consider an equilibrium pair (x_e, u_e) defined through (4). Given $\kappa \in \mathbb{R}_{>0}$ and $v \in \mathbb{R}_{>0}^m$ assume that $\kappa v \leq \min\{u^- + u_e, u^+ - u_e\}$, and let K, L, P_v defined in (8) correspond to an optimal solution of (9). Then the following selection of the input u

$$u = u_e + K(x + A^{-1}Bu_e) + Ldz_{[u^-, u^+]}(u) \quad (11)$$

ensures that function $V_{x_e} : \mathbb{R}^n \rightarrow \mathbb{R}_{\geq 0}$

$$V_{x_e}(x) = (x - x_e)^\top P_v (x - x_e) = |x - x_e|_{P_v}^2 = |\tilde{x}|_{P_v}^2 \quad (12)$$

exponentially decreases with rate larger than 2α within the sublevel set $\tilde{x} \in \mathcal{E}_0^\kappa(P_v)$. Consequently, selection (11) locally exponentially stabilizes the (induced) equilibrium $x_e(u_e)$ of (1) with basin of attraction containing the shifted ellipsoid $\mathcal{E}_{x_e}^\kappa(P_v)$ defined in (7). \square

Remark 1: Expression (11) specifies the control input u only implicitly, even though Proposition 1 ensures that the corresponding solution is Lipschitz. Proceeding as in [10, Lemma 3], for the single-input case $m = 1$, the selection

$$u = u_e + K(x + A^{-1}Bu_e) + L(I - L)^{-1}dz_{[u^-, u^+]}(u_e + K(x + A^{-1}Bu_e))$$

can be proven to be the explicit solution to (11). \circ

Before we conclude this section with an example putting these results into context, we point out that an appropriate coordinate transformation $x \mapsto P_v^{\frac{1}{2}}x$, i.e.,

$$\chi = P_v^{\frac{1}{2}}x \iff x = (P_v^{\frac{1}{2}})^{-1}\chi, \quad (14)$$

with $P_v^{\frac{1}{2}} \in \mathbb{R}^{n \times n}$ symmetric and positive definite, allows us to consider, instead of the Lyapunov function with ellipsoidal level sets, a Lyapunov function with circular level sets, without loss of generality. In particular, using the notation introduced in the results discussed in this section, the function (12) reduces to the Euclidean norm in the χ -coordinates, $\hat{V}_{\chi_e} : \mathbb{R}^n \rightarrow \mathbb{R}_{\geq 0}$, $\hat{V}_{\chi_e}(\chi) = |\chi - \chi_e|^2$. Introducing the vector $C := P_v^{\frac{1}{2}}A^{-1}B$, the set of induced equilibria (4) is given by

$$\chi(u_e) = P_v^{\frac{1}{2}}x_e(u_e) = -P_v^{\frac{1}{2}}A^{-1}Bu_e \quad (15)$$

in the χ -coordinates. While using coordinates χ instead of x is not necessary in the following sections, the interpretations in the χ -coordinates are more illustrative in some places.

Example 1: Consider the dynamical system (1) defined through the matrices $A = \begin{bmatrix} 0.6 & -0.5 \\ 0.3 & 1.0 \end{bmatrix}$ and $B = \begin{bmatrix} 1 \\ 1 \end{bmatrix}$. From (8)¹ the positive definite matrix $P_1 = Q_1^{-1} = \begin{bmatrix} 0.7399 & -0.6654 \\ -0.6654 & 0.8266 \end{bmatrix}$ is obtained for $v = 1$ and $\alpha = 0.1$. In Fig. 1 the level sets of the function $V(x) = x^\top P_1 x$ and $\hat{V}(\chi) = \chi^\top \chi$ are shown on the left and on the right, respectively. Here, we

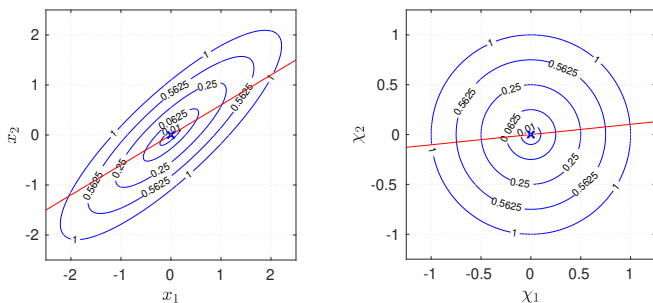


Fig. 1. Level sets of the function $V(x) = x^\top P_1 x$ in the original coordinates (left) and in the rotated coordinates $\chi = P_1^{\frac{1}{2}}x$ (right). Additionally, the subspace of induced equilibria (3) is shown in red.

obtain $P_1^{\frac{1}{2}} = \begin{bmatrix} 0.7447 & -0.4305 \\ -0.4305 & 0.8008 \end{bmatrix}$. In addition, the subspace

¹To avoid numerical problems, the absolute values of unknowns in (8) are additionally constrained to be less or equal to 10. Here, (8) is solved through CVX [4] in Matlab.

of induced equilibria Γ defined in (3) is shown in red in Fig. 1. Since $v = 1$, if $\kappa \leq \min\{u^-, u^+\}$ for $\kappa \in \mathbb{R}_{>0}$, then the origin of the closed-loop system (6) is asymptotically stable and the domain of attraction contains the set $\mathcal{E}_0^\kappa(P_1)$ according to Proposition 1 and Corollary 1.

Assume now that the saturation levels are chosen as $u^- = 1.5$ and $u^+ = 0.5$. Then Proposition 1 and Corollary 1 can be applied with $v = 1$ and $\kappa = 0.5$ guaranteeing that the blue sublevel set in Fig. 2 is contained in the basin of attraction of the closed-loop system (6). Alternatively, the sublevel sets

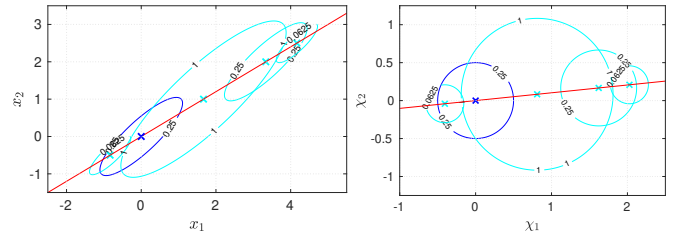


Fig. 2. Sublevel sets $\mathcal{E}_{x_e}^\kappa(P)$ for different (induced) equilibria for which the combination of Proposition 1 and Corollaries 1 and 2 guarantee asymptotic stability of the (induced) equilibrium x_e of the closed loop system.

guaranteeing asymptotic stability of the induced equilibria $x_e = -A^{-1}Bu_e$, $u_e \in (-1.5, 0.5)$, using the feedback law (11) can be derived through Corollary 2. For $u_e = -0.5$, the assumptions of Corollary 2 are satisfied for $\kappa = 1$, leading to a larger sublevel set $\mathcal{E}_{x_e(u_e)}^1(P_1)$, compared with $\mathcal{E}_0^{0.5}(P_1)$, for which convergence to x_e is guaranteed (see Fig. 2). \diamond

III. OPTIMIZATION-BASED SHIFTED STABILIZER

Fig. 2 and the discussions above clearly indicate that the size of the estimate of the region of attraction varies significantly with the induced equilibrium to be stabilized. We exploit here this potential by deriving a modified controller with a larger estimate of the basin of attraction. In particular, the basin of attraction of our modified feedback law includes all sublevel sets $\mathcal{E}_{x_e(u_e)}^\kappa(P_1)$, $u_e \in (-u^-, u^+)$, for which asymptotic stability of x_e is guaranteed through Proposition 1, Corollaries 1 and 2 with the shifted feedback law (11). From this point onwards, we restrict our attention to the single input case, i.e., we assume that $m = 1$.

A. Properties of the shifted stabilizer

Let $P_{\bar{u}}$ be the solution of (8) with $\bar{u} = \mathbb{1}$ defined in (2). Then, the function $\beta : [-u^-, u^+] \rightarrow [0, 1]$ defined as

$$\beta(u_e) = \min\{u^- + u_e, u^+ - u_e\} = \begin{cases} u^- + u_e, & \text{for } u_e \in [-u^-, u_o] \\ u^+ - u_e, & \text{for } u_e \in [u_o, u^+] \end{cases} \quad (16)$$

defines the maximal value $\beta(u_e) = \kappa$ in Corollary 2 (with $v = \bar{u}$) such that the assumptions of Corollary 2 are satisfied. Moreover, according to Corollary 1, the feedback law (11) guarantees the asymptotic stability of $x_e(u_e)$ with region of attraction containing the set

$$\mathcal{E}_{x_e(u_e)}^{\beta(u_e)}(P_{\bar{u}}) = \{x \in \mathbb{R}^n : |x - x_e(u_e)|_{P_{\bar{u}}} \leq \beta(u_e)\}. \quad (17)$$

In the χ -coordinates, introducing $\chi_e(u_e) := P_{\bar{u}}^{\frac{1}{2}} x_e(u_e)$ (see (14)), the set $\mathcal{E}_{x_e(u_e)}^{\beta(u_e)}(P_{\bar{u}})$ simplifies to

$$\mathcal{E}_{\chi_e(u_e)}^{\beta(u_e)}(I) = \{\chi \in \mathbb{R}^n : |\chi - \chi_e(u_e)| \leq \beta(u_e)\}, \quad (18)$$

which we will work with in the following. In this section we will prove that the proposed scheduled law is stabilizing with basin of attraction containing the union of the sublevel sets generated by all possible values of $u_e \in (-u^-, u^+)$,

$$\mathcal{R}_x = \bigcup_{u_e \in (-u^-, u^+)} \mathcal{E}_{x_e(u_e)}^{\beta(u_e)}(P_{\bar{u}}), \quad \mathcal{R}_\chi = \bigcup_{u_e \in (-u^-, u^+)} \mathcal{E}_{\chi_e(u_e)}^{\beta(u_e)}(I), \quad (19)$$

expressed in the x - and χ -coordinates, respectively. For $\chi \in \text{int}(\mathcal{R}_\chi)$ we consider the following optimization problem

$$\begin{aligned} u_e^*(\chi) \in & \underset{u_e \in (-u^-, u^+)}{\text{argmin}} \quad \chi_e(u_e)^\top \chi_e(u_e) \\ & \text{subject to} \quad |\chi - \chi_e(u_e)| \leq \beta(u_e). \end{aligned} \quad (20)$$

Based on a state $\chi \in \text{int}(\mathcal{R}_\chi)$, optimization problem (20) implicitly defines an induced equilibrium pair (χ_e^*, u_e^*) , with

$$\chi_e^* = \chi_e(u_e^*) := P_{\bar{u}}^{\frac{1}{2}} x_e(u_e^*) = -C u_e^* := -P_{\bar{u}}^{\frac{1}{2}} A^{-1} B u_e^* \quad (21)$$

such that $\chi \in \mathcal{E}_{\chi_e^*}^{\beta(u_e^*)}(I)$ holds. Moreover, the objective function is defined so that, from the set of feasible solutions, the one with the shortest distance to the origin is selected.

Lemma 1: Let $m = 1$ and assume that Assumptions 1 and 2 are satisfied. Consider the optimization problem (20) where β and \mathcal{R}_χ are defined in (16) and (19), respectively. Then the following properties are satisfied:

- 1) For all $\chi \in \text{int}(\mathcal{R}_\chi)$, (20) is feasible, the feasible set is convex and its interior is nonempty;
- 2) $u_e^*(\chi) = 0$ for all $\chi \in \mathcal{E}_0^{\beta(0)}(I)$;
- 3) $u_e^*(\chi)$ satisfies $|\chi - \chi_e(u_e^*)| = \beta(u_e^*)$ for all $\chi \in \text{int}(\mathcal{R}_\chi) \setminus \mathcal{E}_0^{\beta(0)}(I)$;
- 4) $u_e^*(\chi) \in (u^-, u^+)$ is unique for all $\chi \in \text{int}(\mathcal{R}_\chi)$; and
- 5) $u_e^*(\cdot) : \text{int}(\mathcal{R}_\chi) \rightarrow (-u^-, u^+)$ is continuous. \lrcorner

Proof: **Item 1.** Feasibility follows immediately from the definition of the function β and the set \mathcal{R}_χ . Moreover, since χ is in the interior of \mathcal{R}_χ , a feasible point can be infinitesimally increased/decreased while remaining feasible. Let $\chi \in \mathcal{R}_\chi$ and take $u_{e_1}, u_{e_2} \in (-u^-, u^+)$ such that $|\chi - \chi_e(u_{e_1})| \leq \beta(u_{e_1})$ and $|\chi - \chi_e(u_{e_2})| \leq \beta(u_{e_2})$. Then for all $\lambda \in [0, 1]$ it holds that

$$\begin{aligned} & |\chi - \chi_e(\lambda_1 u_{e_1} + (1 - \lambda) u_{e_2})| \\ & \leq \lambda |\chi - \chi_e(u_{e_1})| + (1 - \lambda) |\chi - \chi_e(u_{e_2})| \\ & \leq \lambda \beta(u_{e_1}) + (1 - \lambda) \beta(u_{e_2}) \leq \beta(\lambda u_{e_1} + (1 - \lambda) u_{e_2}). \end{aligned}$$

The last step follows from the concavity of β in (16).

Item 2. The second item follows immediately from (18) together with the objective function.

Item 3. Assume that $|\chi - \chi_e(u_e^*)| < \beta(u_e^*)$. Since $\chi \notin \mathcal{E}_0^{\beta(0)}(I)$ it follows that $\chi_e(u_e^*) \neq 0$, i.e., $u_e^* \neq 0$. Since $\beta(\cdot)$, $\chi_e(\cdot)$ and $|\cdot|$ are continuous functions, there exists $u_e^\# \in (-u^-, u^+)$ with $|u_e^\#| < |u_e^*|$ and $|\chi - \chi_e(u_e^\#)| < \beta(u_e^\#)$. Moreover, the condition $|u_e^\#| < |u_e^*|$ implies that

$\chi_e(u_e^\#)^\top \chi_e(u_e^\#) < \chi_e(u_e^*)^\top \chi_e(u_e^*)$, which contradicts the optimality of u_e^* and thus completes the proof.

Item 4. For $\chi \in \mathcal{E}_0^{\beta(0)}(I)$ it holds that $u_e^* = 0$ and $\chi(u_e^*) = 0$ and thus uniqueness follows since the objective function satisfies $|\chi_e(u_e)|^2 = 0$ if and only if $u_e = 0$. Consider now $\chi \in \text{int}(\mathcal{R}_\chi) \setminus \mathcal{E}_0^{\beta(0)}(I)$ and let u_e^{*1}, u_e^{*2} with $u_e^{*1} \neq u_e^{*2}$ denote two optimal solutions. Due to the objective function and the fact that $\chi_e = -P_{\bar{u}}^{\frac{1}{2}} A^{-1} B u_e$, it holds that $u_e^{*1} = -u_e^{*2}$ and the origin can be defined as the average $u_e^\# = 0 = \frac{1}{2}(u_e^{*1} + u_e^{*2})$. Since β in (16) is a concave function, then it holds that $\min\{\beta(u_e^{*1}), \beta(u_e^{*2})\} \leq \beta(u_e^\#) = \beta(0)$, i.e., $\chi \in \mathcal{E}_0^{\beta(0)}(I)$, which implies that the optimal solution is $\chi_e^* = -P_{\bar{u}}^{\frac{1}{2}} A^{-1} B u_e^\# = 0$, thus contradicting the optimality of u_e^{*1}, u_e^{*2} .

Item 5. Note that in the domain of interest $\chi \in \text{int}(\mathcal{R}_\chi)$, $u_e \in (-u^-, u^+)$, the constraints in (20) coincide with non-positivity of the two continuously differentiable functions $g_1(\chi, u_e) = |\chi + C u_e|^2 - (u^- + u_e)^2$ and $g_2(\chi, u_e) = |\chi + C u_e|^2 - (u^+ - u_e)^2$. Continuity of $u_e^*(\cdot)$ then follows from [11, Lemma 5.3(b)] and [11, Lemma 5.4(b)] which establish lower and upper semicontinuity of $u_e^*(\cdot)$, respectively. The assumptions of [11, Lemma 5.3(b)] are satisfied since $u_e^*(\cdot)$ is restricted to the bounded domain $u_e^*(\cdot) \in [-u^-, u^+]$ (see property LC on [11, Page 52]). The assumptions of [11, Lemma 5.4(b)] are satisfied since the constraint qualification (CQ) (see [11, Definition 5.3]) holds because the feasible set is convex with nonempty interior (see item 1). \blacksquare

Remark 2: Lemma 1 establishes continuity of u_e^* . Establishing stronger Lipschitz continuity is an open problem, in general, even though geometrical considerations suggest that Lipschitz continuity does not hold when $|C| = 1$. \circ

B. Stabilization with scheduled shifted coordinates

With Lemma 1 we are able to construct a control law stabilizing the origin from any initial condition satisfying $x \in \text{int}(\mathcal{R}_x)$. Recall that, through the coordinate transformation (14), there is a one to one mapping between x and χ , therefore we can equivalently express the control law as a function of χ or x . Opting for the formulation as a function of x , we can now state the main feedback controller proposed in this paper, combining the results of Corollary 2 and Lemma 1 (together with Remark 1 for the case $m = 1$ addressed here). The controller is given by the state feedback law

$$\begin{aligned} u = & u_e^*(x) + K(x + A^{-1} B u_e^*(x)) \\ & + L(I - L)^{-1} dz_{[u^-, u^+]}(u_e^*(x) + K(x + A^{-1} B u_e^*(x))), \end{aligned} \quad (22)$$

defined through the optimal solution of (20). Based on Lemma 1, our main theorem proves its properties.

Theorem 1: Consider system (1) with $m = 1$, satisfying Assumptions 1 and 2. Let $u^-, u^+ \in \mathbb{R}_{>0}$, let $P_{\bar{u}}$ denote the solution of (8) for $v = \bar{u}$ and $\alpha > 0$ arbitrary. Then the feedback control law (22)

- 1) is well defined and continuous for all $x \in \text{int}(\mathcal{R}_x)$;
- 2) asymptotically stabilizes the origin of (1), and the basin of attraction contains the set $\text{int}(\mathcal{R}_x)$. \lrcorner

Proof: The proof exploits Lemma 1. The equivalence between the coordinate representations χ and x allows us to apply the results of Lemma 1 also in the x coordinates.

Item 1. The property that (22) is well defined in $x \in \text{int}(\mathcal{R}_x)$ and continuity of the feedback law follow immediately from the corresponding properties in Lemma 1.

Item 2. First note that, through the second item in Lemma 1, in the set $\mathcal{E}_0^{\beta(0)}(P_{\bar{u}})$, the modified control law (22) and the original control law (5) coincide. Thus the origin is Lyapunov stable and $\mathcal{E}_0^{\beta(0)}(P_{\bar{u}})$ is contained in the region of attraction of the origin. Moreover, for $x \in \text{int}(\mathcal{R}_x)$ the control law (22) coincides with (11), and thus it stabilizes the reference point $x_e(u_e^*) = -A^{-1}Bu_e^*$. Note that by construction $x \in \mathcal{E}_{x_e(u_e^*)}^{\beta(u_e^*)}(P_{\bar{u}})$. Since $\mathcal{E}_{x_e(u_e^*)}^{\beta(u_e^*)}(P_{\bar{u}})$ denotes the sublevel set of $V_{x_e(u_e^*)}(\cdot)$ defined in (12), given any closed-loop solution $x(\cdot)$ and for all t , the distance to $x(t) - x_e(u_e^*(x(t)))$ in terms of the norm $t \mapsto |x(t) - x_e(u_e^*(x(t)))|_{P_{\bar{u}}}$ is contractive with rate at least $2\alpha > 0$. Contractivity implies that any solution starting in $\text{int}(\mathcal{R}_x)$ satisfies $x(t) \in \text{int}(\mathcal{R}_x)$ for all $t \geq 0$. Furthermore, the contractivity of the boundary of $\mathcal{E}_{x_e(u_e^*)}^{\beta(u_e^*)}(P_{\bar{u}})$, together with the selection of the objective function in (20) implies that $t \mapsto |x_e(x(t))|$ is a decreasing function.

It is left to show that $|x_e(u_e^*(x(t)))| = 0$ is satisfied for $t \in \mathbb{R}_{\geq 0}$ sufficiently large. Assume, for the sake of a contradiction, that $x_e(u_e^*(x(t))) \rightarrow x_e^\# \neq 0$ for $t \rightarrow \infty$. In this case $x(t) \rightarrow x_e^\#$ for $t \rightarrow \infty$ according to the definition and the properties of the control law (11). However, the fact that $\beta(x_e^\#) > 0$ together with the selection of the objective function in (20) implies that $|x_e(u_e^*(x(t)))| < |x_e^\#|$ for $t \in \mathbb{R}_{\geq 0}$ sufficiently large, leading to a contradiction. ■

Remark 3: Based on Theorem 1, it is possible to show that the continuous function $W : \mathcal{R}_x \rightarrow \mathbb{R}_{\geq 0}$ defined as

$$W(x) = \frac{|x - x_e(u_e^*(x))|_{P_{\bar{u}}}^2}{\beta(u_e^*(x))^2} + (u_e^*(x))^2 \quad (23)$$

is a Lyapunov-like function for the closed-loop system. Indeed W satisfies quadratic upper and lower bounds in \mathcal{R}_x and decreases along the solutions of (1), (22). However, function W would certify local asymptotic stability only if u_e^* is Lipschitz, which does not seem to be true in general. ◦

In the proof of Theorem 1, we have exploited the fact that the original feedback law (5) and the modified feedback law (22) are the same in a neighborhood around the origin. This implies that performance is locally preserved, which we state for completeness in the following corollary. This result could not be attained by the asymmetric solution proposed in [10], due to the convex scaling performed therein, which reduced by one half the convergence rate (see [3, Thm 3.3]).

Corollary 3: Let the assumptions of Theorem 1 be satisfied. For $x \in \mathcal{E}_0^{\beta(0)}(P_{\bar{u}})$, controller (22) coincides with controller (5), thus locally preserving the performance. ◻

IV. EXPLICIT EXPRESSION OF THE STABILIZER

So far the feedback law (22) is only implicitly defined through the optimal solution of (20). However, due to the

simplicity of the optimization problem in the single input case, a finite set of possible optimal solutions can be derived offline, from which the selection of the optimal solution online is straightforward. To present the corresponding result we use the quantity C defined in (21) and define u_e^* in terms of χ instead of x . Additionally, we define $u_e^{\#i} \in \mathbb{C} \cup \{\pm\infty\}$, $i \in \{1, \dots, 6\}$ with

$$\begin{aligned} u_e^{\#1}(\chi) &= \frac{-|\chi|^2 + (u^-)^2}{2(\chi^\top C - u^-)}, & u_e^{\#2}(\chi) &= \frac{-|\chi|^2 + (u^+)^2}{2(\chi^\top C + u^+)}, \\ u_e^{\#3,4}(\chi) &= \frac{\chi^\top C - u^- \pm \sqrt{(\chi^\top C)^2 - |C|^2|\chi|^2 + |Cu^- - \chi|^2}}{1 - |C|^2}, \\ u_e^{\#5,6}(\chi) &= \frac{\chi^\top C + u^+ \pm \sqrt{(\chi^\top C)^2 - |C|^2|\chi|^2 + |Cu^+ + \chi|^2}}{1 - |C|^2}. \end{aligned}$$

Theorem 2: Let the assumptions of Theorem 1 be satisfied and consider the optimization problem (20) and C defined in (21). If $|C| = 1$ define

$$\mathcal{S} = (\{u_e^{\#1}\} \cap [-u^-, u_0]) \cup (\{u_e^{\#2}\} \cap [u_0, u^+])$$

and for $|C| \neq 1$ consider

$$\mathcal{S} = (\{u_e^{\#3}, u_e^{\#4}\} \cap [-u^-, u_0]) \cup (\{u_e^{\#5}, u_e^{\#6}\} \cap [u_0, u^+]).$$

Then, for $\chi \in \text{int}(\mathcal{R}_x) \setminus \mathcal{E}_0^{\beta(0)}(I)$, the optimal solution of (20) satisfies

$$u_e^*(\chi) \in \text{argmin}_{u_e \in \mathcal{S}} |\chi_e(u_e)|^2. \quad (24)$$

Moreover, for $\chi \in \mathcal{E}_0^{\beta(0)}(I)$ the optimal solution of (20) is given by $u_e^* = 0$. ◻

Note that the set \mathcal{S} , which can be easily constructed, contains at most 4 points. Thus, the optimal solution of (20) is obtained by calculating and comparing the objective values of $u_e \in \mathcal{S}$ in (24).

Proof: The fact that $u_e^*(\chi) = 0$ for $\chi \in \mathcal{E}_0^{\beta(0)}(I)$ follows from Lemma 1, item 2. The six values $u_e^{\#i}(\chi)$, $i \in \{1, \dots, 6\}$ are obtained by solving the constraint

$$|\chi - \chi_e(u_e)|^2 = (\beta(u_e))^2 \quad (25)$$

of the optimization problem (20) for $\beta(u_e) = u^- + u_e$ and $\beta(u_e) = u^+ - u_e$ according to the definition of β in (16). The consideration of equality instead of inequality in (25) is justified through Lemma 1, item 3. It follows from standard calculations that $u_e^{\#i}(\chi)$, $i \in \{1, 2\}$, represent the solutions of (25) in the case $|C| = 1$ while $u_e^{\#i}(\chi)$, $i \in \{3, \dots, 6\}$ are the solutions of (25) in the case $|C| \neq 1$. Since Lemma 1, item 1, guarantees that $\mathcal{S} \neq \emptyset$, the assertion follows. ■

V. NUMERICAL ILLUSTRATION

Example 2: We continue with the setting discussed in Example 1. The closed-loop solutions using the feedback law (22) initialized at $x_0 = [4.8, 3]^\top$ and $x_0 = [-1.6, -0.96]^\top$ are shown in Fig. 3. The areas \mathcal{R}_x and \mathcal{R}_χ , respectively, for which convergence to the origin is guaranteed are shown in cyan. The areas $\mathcal{E}_0^{\beta(0)}(P_1)$ and $\mathcal{E}_0^{\beta(0)}(I)$ corresponding to Proposition 1 are shown in blue. Even though not represented in our figures, the solutions corresponding to the initial

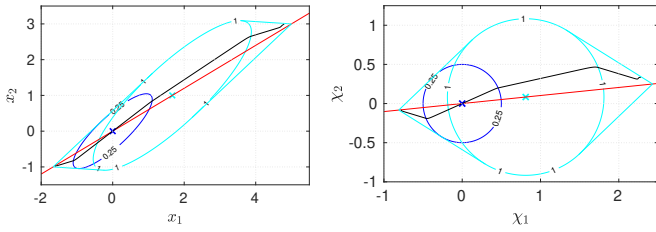


Fig. 3. Closed loop solutions using the feedback law (22) converging to the origin (black). Additionally, \mathcal{R}_x and \mathcal{R}_y (cyan), $\mathcal{E}_0^{\beta(0)}(P_1)$ and $\mathcal{E}_0^{\beta(0)}(I)$ (blue) and the subspace of induced equilibria Γ (red) are shown.

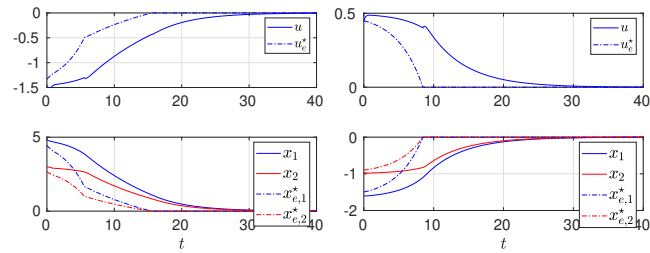


Fig. 4. Evolution of input u , state x and points u_e and x_e for the initial conditions $x_0 = [4.8, 3]^T$ (left) and $x_0 = [-1.6, -0.96]^T$ (right). The kink occurs when the slope of $\beta(u_e)$ changes from increasing to decreasing (left) and when the state x enters the set $\mathcal{E}_0^{\beta(0)}(P_1)$ (right).

conditions $x_0 = [4.8, 3]^T$ and $x_0 = [-1.6, -0.96]^T$ using the original control law (5) are diverging. The time evolution of the input u and the state x is visualized in Fig. 4, which also shows the evolution of the reference points u_e and x_e .

Fig. 5 illustrates the observation of Remark 3 through the level sets of function W in (23), for this example, together with its decrease along the closed-loop solutions.

Example 3: To illustrate that our solution applies with any state dimension $n \in \mathbb{N}$, consider plant (1) with

$$A = \begin{bmatrix} 0.6 & -0.8 & 0.3 \\ 0.8 & 0.6 & 0.5 \\ 1.0 & 0.3 & -1.0 \end{bmatrix} \quad \text{and} \quad B = \begin{bmatrix} 1 \\ 4 \\ 2 \end{bmatrix}. \quad (26)$$

Similar to the two-dimensional case in Figs. 3 and 4, estimates of the region of attraction and a closed-loop solution are visualized in Fig. 6. The control law is again obtained by solving (8)² for $v = 1$ and $\alpha = 0.1$ and the saturation levels are defined as $u^- = 1.5$ and $u^+ = 0.5$. The closed-loop solution shown in Fig. 6 is initialized at $x_0 = [3.5, 1.5, 2.5]^T$.

VI. CONCLUSIONS

Through a suitably scheduled shift of the equilibrium, an enlarged estimate of the basin of attraction for bounded control laws with asymmetric saturations has been obtained. The control law is implicitly defined through an optimization problem. The focus on the single input setting enables an illustrative interpretation of the controller design and allows for an explicit representation of the control law.

Future work will address the multi input case and remove the assumption that A be non-singular, by directly representing Γ through the kernel of $[A, B]$. To be able to derive explicit solutions of (20) in the multi input setting, the

²As in Example 1, the absolute values of the unknowns are constrained to be less than or equal to 10.

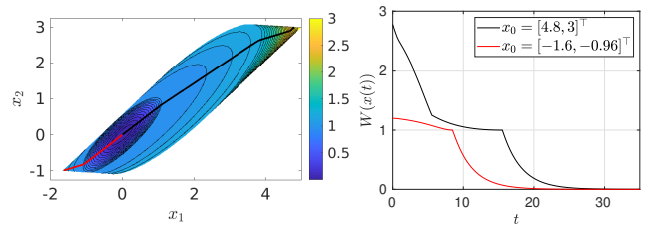


Fig. 5. Example 2: Level sets of the function W in (23) for the dynamics defined in Example 1 and decrease of W along the solutions of (1), (22).

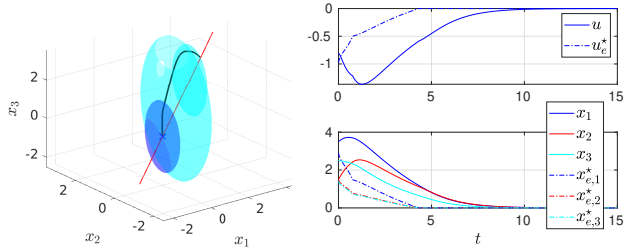


Fig. 6. Example 3: Estimates of the region of attraction and a closed-loop solution using the feedback law (22) for dynamics (26).

optimization problem may be reduced to a one dimensional subspace in the kernel of $[A, B]$, depending on the state position. Alternatively, sample-and-hold approaches may be investigated, where equilibrium pairs (x_e^*, u_e^*) are only updated at discrete time steps.

REFERENCES

- [1] A. Benzaouia. Constrained stabilization: an enlargement technique of positively invariant sets. *IMA Journal of Mathematical Control and Information*, 22(1):109–118, 2005.
- [2] A. Benzaouia, F. Mesquine, and M. Benhayoun. *Saturated Control of Linear Systems*. Springer, 2017.
- [3] F. Blanchini and S. Miani. Any domain of attraction for a linear constrained system is a tracking domain of attraction. *SIAM Journal on Control and Optimization*, 38(3):971–994, 2000.
- [4] M. Grant and S. Boyd. CVX: Matlab software for disciplined convex programming, version 2.1. <http://cvxr.com/cvx>, 2014.
- [5] B.L. Groff, J.M. Gomes da Silva Jr, and G. Valmorbid. Regional stability of discrete-time linear systems subject to asymmetric input saturation. *IEEE Conf. on Decision and Control*, pages 169–174, 2019.
- [6] T. Hu and Z. Lin. *Control systems with actuator saturation: analysis and design*. Springer Science & Business Media, 2001.
- [7] T. Hu, A.N. Pitsillides, and Z. Lin. Null controllability and stabilization of linear systems subject to asymmetric actuator saturation. In *IEEE Conf. on Decision and Control*, pages 3254–3259, 2000.
- [8] T. Hu, A.N. Pitsillides, and Z. Lin. Null controllability and stabilization of linear systems subject to asymmetric actuator saturation. In V. Kapila and K. Grigoriadis, editors, *Actuator Saturation Control*, chapter 1, pages 47–76. Marcel Dekker, 2002.
- [9] Y. Li and Z. Lin. An asymmetric Lyapunov function for linear systems with asymmetric actuator saturation. *International Journal of Robust Nonlinear Control*, 21(4):1–17, 2017.
- [10] S. Mariano, F. Blanchini, S. Formentin, and L. Zaccarian. Asymmetric state feedback for linear plants with asymmetric input saturation. *IEEE Control Systems Letters*, 4(3):608–613, 2020.
- [11] G. Still. Lectures on parametric optimization: An introduction. *Optimization Online*, 2018.
- [12] S. Tarbouriech, G. Garcia, J.M. Gomes da Silva Jr, and I. Queinnec. *Stability and stabilization of linear systems with saturating actuators*. Springer-Verlag London Ltd., 2011.
- [13] C. Yuan and F. Wu. Switching control of linear systems subject to asymmetric actuator saturation. *International Journal of Control*, 88(1):204–215, 2015.